

## A QUBO Formulation for Eigencentality

**Prosper D. Akrobotu** ·  
**Tamsin E. James** ·  
**Christian F. A. Negre** ·  
**Susan M. Mniszewski**

Received: date / Accepted: date

**Abstract** The efficient calculation of the centrality or “hierarchy” of nodes in a network has gained great relevance in recent years due to the generation of large amounts of data. The eigenvector centrality is quickly becoming a good metric for centrality due to both its simplicity and fidelity. In this work we lay the foundations for the calculation of eigenvector centrality using quantum computational paradigms such as quantum annealing and gate-based quantum computing. The problem is reformulated as a quadratic unconstrained binary optimization (QUBO) that can be solved on both quantum architectures. The results focus on correctly identifying a given number of the most important nodes in numerous networks given by our QUBO formulation of eigenvector centrality on both the D-Wave and IBM quantum computers.

**Keywords** Eigenvector Centrality · Quantum Annealing · Quadratic Unconstrained Binary Optimization · Gate-Based Quantum Computing

---

Prosper D. Akrobotu  
Department of Mathematical Sciences  
The University of Texas at Dallas  
Richardson, TX 75080  
E-mail: prosper.akrobotu@utdallas.edu

Tamsin E. James  
E-mail: tamsin.j@hotmail.co.uk

Christian F. A. Negre  
Theoretical Division  
Los Alamos National Laboratory  
Los Alamos, NM 87545  
E-mail: cnegre@lanl.gov

Susan M. Mniszewski (Corresponding author)  
Computer, Computational, and Statistical Sciences Division  
Los Alamos National Laboratory  
Los Alamos, NM 87545  
E-mail: smm@lanl.gov

## 1 Introduction

There are several centrality measures used to identify the most influential node or nodes within a network, each having their own benefits dependent on the data at hand or the results desired.

For example, degree centrality [1], which is based purely on the number of connections a node has, could be used for identifying the most popular person within a group of people on a social media platform (number of followers). Closeness centrality [2] is dependent on the length of the paths from one node to all other nodes in a network, prioritizing nodes that are “closer” to all other nodes as more central. This has been used for predicting enzyme catalytic residues from topological descriptions of protein structures [3]. Betweenness centrality [4], is based on the number of times a node appears when two other nodes are connected by their shortest path. This measure is often used in biological networks, for example identifying a specific protein that is important for information flow within a network, which could be used in drug discovery [5]. Katz centrality [6], measures the importance of a node through its immediate connections, and also the connections of other nodes through the immediate neighbors. Katz centrality has also been used within a biological setting, such as identifying disease genes [7]. PageRank centrality [8] is a variant of eigenvector centrality designed to rank web pages by importance based on links between pages or articles. This differs from eigenvector centrality as it takes into account directions between nodes (clicking from one web page to another).

It is worth noting at this point that the rankings generated by these different centrality measures are correlated, especially for the most highly ranked nodes [9, 10, 11, 12, 13]. Our research is concentrated on a study of the eigenvector centrality (EC) measure [14], and using this to determine the most important nodes in a given network. EC has been applied in many different fields of science. For example, identifying the most important amino acid residues in proteins undergoing an allosteric mechanism [15] and predicting flow-paths in porous materials [16]. It is also relevant to current world issues related to the COVID-19 pandemic, such as identifying people deemed as “super-spreaders” and areas that are hot-spots in a pandemic (network of people) [17], and also in the analysis of production chains in the financial market, where micro-sectors are identified as important nodes within a chain [18].

EC is a centrality measure which assigns to each node a value that is proportional to the sum of the values for the node’s neighbors [19, 15]. With this measure, the most influential node is a node that is connected to a majority of the other important nodes in the network. The scheme designed to implement the EC measure starts by obtaining the network’s adjacency matrix, a matrix that describes the network’s connectivity and is defined as follows: Let  $A = [a_{ij}]_{n \times n}$  be the adjacency matrix of a network or graph  $G = (V, E)$  of  $n$

nodes with entries defined by

$$a_{ij} = \begin{cases} 1 & \{u_i, u_j\} \in E \text{ for } u_i, u_j \in V \\ 0 & \text{otherwise} \end{cases}$$

where  $E$  is the set of edges and  $V$  is the set of nodes or vertices. The Perron-Frobenius theorem[20] states that there is a unique largest real eigenvalue for a non-negative square matrix (here given by the adjacency matrix), with an eigenvector solution consisting of positive elements. So let the largest eigenvalue of  $A$  be  $\lambda_1$ . Then the EC measure assigns to each node the value

$$x_i = \frac{1}{\lambda_1} \sum_{j=1}^n a_{ij} x_j \quad \forall i = 1, 2, \dots, n \quad (1)$$

where  $x_i$  is the given centrality value for the  $i^{\text{th}}$  node. It is represented in matrix form by

$$A\mathbf{x} = \lambda_1\mathbf{x} \quad (2)$$

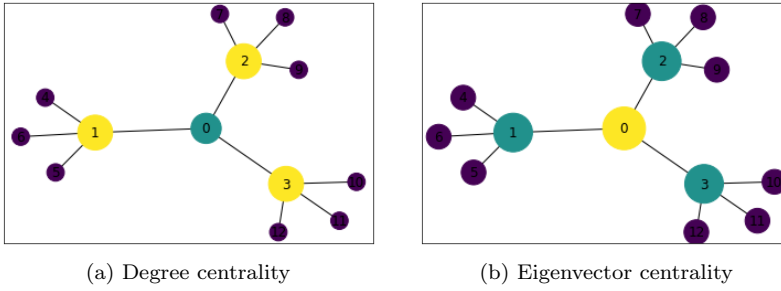


**Fig. 1** Identifying the importance of a node in a network based on (a) degree centrality and (b) eigenvector centrality. The color and radius of each disk around a node is dependent upon the centrality values. The least central nodes are colored in purple, the mid-central nodes are colored in green with the most central nodes colored yellow. Nodes 1, 2 and 3 have the highest values when using the degree centrality measure while node 0 has the highest value when using the EC measure.

The degree centrality can also be defined as the count of the number of walks of length one that reach the node for which centrality is being computed. EC instead, is a count of the number of walks of infinite length [14, 9]. A brief demonstration of these concepts are shown in the Appendix with details also found in [10].

Due to the number of uses of centrality measures, it appears to be a good step forward to reformulate these problems for use on quantum computers. As networks become larger and more complicated, such as in drug discovery, the use of quantum computers could prove to be of great help in the future.

Our research seeks to reformulate the iterative scheme for the EC problem as a classical optimization problem and encode it as a quadratic unconstrained binary optimization (QUBO) problem for quantum computers.

The steady progress in the field of quantum computing since its proposal in the early 1980s by Richard Feynman, has seen researchers trying different directions to circumvent the complexity of constructing portable physical quantum computers. Currently, there are two major approaches for building quantum computers: gate-based and quantum annealing. The gate-based quantum computers are designed using quantum circuits with control and manipulative power over the evolution of quantum states to tackle general problems arising in nature [21, 22]. The quantum annealing approach, however, uses the natural evolution of quantum states to tackle specific problems such as probabilistic sampling and combinatorial optimization problems [22].

The D-Wave quantum computer is a quantum computing platform that uses quantum annealing (QA), a heuristic search method that makes use of quantum tunneling and quantum entanglement to solve the ground state of the Ising model equivalence of combinatorial optimization problems. That is, any problem to be solved by the D-Wave quantum annealer, is to be modeled as a search for the minimum energy of the Ising Hamiltonian energy function as follows.

$$E(\mathbf{s}) = \sum_i h_i s_i + \sum_{i < j} J_{i,j} s_i s_j \quad (3)$$

where  $s_i \in \{-1, 1\}$  are magnetic spin variables subject to local fields  $h_i$  and nearest neighbor interactions with coupling strength  $J_{ij}$  or its Boolean equivalence obtained from the transformation  $\mathbf{s} = 2\mathbf{x} - \mathbf{1}$  where the entries of the vector  $\mathbf{x}$  represent the binary variables  $x_i \in \{0, 1\}$  and  $\mathbf{1}$  is a vector of ones. The Boolean equivalence of the Ising problem is referred to as a QUBO problem, with the following equation

$$E(\mathbf{x}) = \mathbf{x}^T Q \mathbf{x} = \sum_{i=1}^N x_i Q_{ii} + \sum_{i \neq j} x_i x_j Q_{ij}. \quad (4)$$

D-Wave quantum annealers include the current 2000Q and the new **Advantage** [23]. The quantum processing unit (QPU) of the D-Wave 2000Q has up to 2048 qubits and 6061 couplers sparsely connected as a Chimera graph  $C_{16}$  [23]. While the **Advantage** consists of more than 5000 superconducting qubits connected with 35,000 couplers on a Pegasus graph [23]. The sparse connectivity of the chimera graph of the D-Wave 2000Q requires a “minor embedding” of the Ising model connectivity of the problem onto the hardware. This results in chains of physical qubits representing logical qubits leading to a maximum capacity of 64 fully connected logical qubits/variables [24]. The D-Wave quantum computers possess the ability to sample degenerate ground state solutions and have been utilized in solving several problems such as quantum isomer search [25], graph partitioning [26], community detection [27], binary clustering [28], graph isomorphism [29] and classifier [30, 31]. It

has also been used in solving physical problems related to atomistic configuration stability [32], job-shop scheduling [33], airport and air traffic management [34, 35].

The gate-based quantum computers use unitary operations defined on a quantum circuit to transform input data into a desired output data [21, 36]. This computational mechanism is employed in the design of IBM quantum computers which are made available through a cloud-based platform called IBM Quantum (IBM-Q) Experience [37]. The unitary operations are designed to process data with high fidelity and to tackle both combinatorial optimization problems and non-combinatorial problems like prime factorization [21]. IBM-Q consists of both quantum hardware and simulators. The basic steps to follow in carrying out any experiment on the IBM-Q Experience requires first to specify a quantum circuit via a graphic interface called composer or a text-based editor (the cloud version is called quantum lab), then run the circuit on a simulator to verify specifications, and finally execute the circuit on the quantum processor for a number  $N$  of shots with  $N = 8192$  being the maximum allowed on current devices [36].

In this paper, our main goal is to reformulate the EC problem as a QUBO problem that correctly identifies a desired number of the most important nodes of an undirected graph when solved on quantum annealing and gate-based quantum computers. As a secondary objective, we probe the possibility of using our formulation to generate a ranking of the nodes that correspond to the rankings obtained via the usual iterative method of solving the EC problem.

The paper is organized as follows. Section 2 elaborates on our extraction of an optimization problem out of the EC problem classically. We then construct a QUBO formulation for identifying a number of the most important nodes of the graph by the EC measure to be implemented on quantum computing devices. Section 3 presents the software tools, implementations and results obtained from the classical and quantum computers such as D-Wave 2000Q and IBM-Q. It also stipulates ways of defining a rank from the results obtained from solving the QUBO on D-Wave 2000Q and provides discussions on the conclusions derived from the results. In section 4, we provide a summary of the results and conclude with suggestions of future directions to be considered.

## 2 Methods

In this section we present the mathematical formulation of the EC problem as an optimization problem. A careful examination of the scheme in Eq (1) and Eq (2) shows that the EC is a problem of determining the eigenvector corresponding to the leading eigenvalue of the adjacency matrix of the network. To this end, we recall some useful properties for the leading eigenvalue of a symmetric matrix.

$$- \frac{x^T Ax}{x^T x} \leq \lambda_1 \leq d_{max}, \text{ where } d_{max} \text{ is the maximum degree of the graph.}$$

Hence it is understood that the maximum of the set of numbers  $\{\frac{\mathbf{x}^T A \mathbf{x}}{\mathbf{x}^T \mathbf{x}}\}$  coincides with the leading eigenvalue of the adjacency matrix and thus one can construct a maximization problem from this property as follows:

$$\max_{\mathbf{x} \in \mathbb{R}^n} \mathbf{x}^T A \mathbf{x} \quad \text{s.t.} \quad \|\mathbf{x}\| = 1 \quad (5)$$

This maximization problem is a constrained optimization problem which is equivalent to the following unconstrained minimization problem:

$$\min_{\mathbf{x} \in \mathbb{R}^n} \left[ -\mathbf{x}^T A \mathbf{x} + P \left( \sum_{i=1}^n x_i^2 - 1 \right)^2 \right] \quad (6)$$

where  $P$  is the Lagrange multiplier or simply a penalty constant and we have used the fact that  $1 = \|\mathbf{x}\|^2 = \sum_{i=1}^n x_i^2$ . The goal here is that the argument of a typical solution to the unconstrained minimization problem should preserve the ranking on the nodes in the network when the usual iterative scheme Eq (2) is used in determining the importance of a node. That is, we are more interested in the rank assigned than the centrality values assigned to each node in the network.

## 2.1 Eigenvector centrality as a QUBO problem

Our goal in this section is to reformulate EC as a QUBO problem. The word “binary” suggests that our search domain must be a binary field, however the original problem requires a search space of real vector spaces. Thus to efficiently transition into binary fields, we will consider simply splitting the set of nodes into two categories: most central and least central, where a value of 1 denotes a node is most central and a value of 0 denotes a node is least central. To this end, we define  $\tau$  as the number of most central nodes we wish to be identified from the set of nodes (i.e. how many nodes are to be assigned the value of 1). The problem of splitting into two categories is binary as we only have two categories: 0 and 1, or high and low. The value  $\tau$  therefore must be chosen with consideration of factors such as the size of the network and how many important nodes you wish to identify. This definition will require a slight modification to our unconstrained minimization model, Eq (6) and a need for more constraints. Now, consider the second term in Eq (6), since the search field is now binary, we have for each  $i$ ,  $x_i^2 = x_i$  and based on the definition of  $\tau$ ,  $\sum_{i=1}^n x_i = \tau$ , we adapt the following modification to the penalty term.

$$P \left( \sum_{i=1}^n x_i^2 - 1 \right)^2 \mapsto P \left( \sum_{i=1}^n x_i - \tau \right)^2 \quad (7)$$

We now write the modified penalty term in matrix notation.

$$\begin{aligned}
\left(\sum_{i=1}^n x_i - \tau\right)^2 &= \left(\sum_{i=1}^n x_i\right)^2 - 2\tau \sum_{i=1}^n x_i + \tau^2 \\
&= \sum_{i=1}^n x_i^2 + 2 \sum_{i<j} x_i x_j - 2\tau \sum_{i=1}^n x_i + \tau^2 \\
&= (1 - 2\tau) \sum_{i=1}^n x_i^2 + 2 \sum_{i<j} x_i x_j + \tau^2 \\
&= \mathbf{x}^T [(1 - 2\tau)I + U] \mathbf{x} + \tau^2 \\
&= \mathbf{x}^T C \mathbf{x} + \tau^2 \tag{8}
\end{aligned}$$

where we have used the fact that  $x_i = x_i^2$  and  $C = (1 - 2\tau)I + U$ ,  $I$  the  $n \times n$  identity matrix and  $U = [u_{ij}]$  is an  $n \times n$  matrix with entries  $u_{ij}$  defined by

$$u_{ij} = \begin{cases} 1 & i \neq j \\ 0 & \text{otherwise} \end{cases} \tag{9}$$

We now attempt to build a problem Hamiltonian from the eigenvector equation, Eq (2). Note that

$$\begin{aligned}
(A\mathbf{x} - \lambda_1\mathbf{x})^2 &= [(A - \lambda_1 I)\mathbf{x}]^T [(A - \lambda_1 I)\mathbf{x}] \\
&= \mathbf{x}^T (A - \lambda_1 I)^T (A - \lambda_1 I) \mathbf{x} \\
&= \mathbf{x}^T A^T A \mathbf{x} - 2\lambda_1 \mathbf{x}^T A \mathbf{x} + \lambda_1^2 \mathbf{x}^T \mathbf{x} \\
&= \mathbf{x}^T A^T A \mathbf{x} - 2d_{max} \mathbf{x}^T A \mathbf{x} + d_{max}^2 \mathbf{x}^T \mathbf{x} + \text{error} \\
&= \mathbf{x}^T A^2 \mathbf{x} - 2d_{max} \mathbf{x}^T A \mathbf{x} + d_{max}^2 \mathbf{x}^T \mathbf{x} + \text{error} \tag{10}
\end{aligned}$$

where we have used  $A^T = A$  for undirected graphs. Naturally, one would expect the optimal solution to an optimization problem with objective function given by Eq (10) to correspond to the desired solution of our problem. However numerical solutions showed otherwise. The solution was mostly found in the excited states and not the ground state. Therefore to ensure the solution to our problem is always embedded in the ground state we modified the objective function slightly to obtain

$$Q = -P_0 A^2 \hat{\mathbf{d}} \hat{\mathbf{d}}^T A - P_0 A \hat{\mathbf{d}} \hat{\mathbf{d}}^T A^2 + P_1 C \tag{11}$$

where  $P_0, P_1$  are penalty constants such that  $P_1 > P_0$ , and

$$\mathbf{d} = \sum_i^n d_i \mathbf{e}_i \text{ where } d_i = \sum_{j=1}^n \mathbf{e}_i^T A \mathbf{e}_j, \text{ and } \hat{\mathbf{d}} = \frac{\mathbf{d}}{\|\mathbf{d}\|} \tag{12}$$

as a replacement for the expression on the righthandside of Eq (10). Here the vectors  $\mathbf{e}_i \in \mathbb{R}^n$  are the canonical basis vectors of  $\mathbb{R}^n$ . We minimize over all the state vectors of the nodes,  $\mathbf{x} \in \{0, 1\}^n$ , of the graph  $G$  and numerically verify the proposition :

**Proposition 1** *Let  $G = (V, E)$  be an undirected graph with  $n = |V|$  nodes, adjacency matrix  $A$  and degree sequence  $\mathbf{d} = (d_1, d_2, \dots, d_n) \in \mathbb{R}^n$ . Using the EC measure, the most central node of the graph  $G$  is the ground state of the QUBO problem.*

$$\begin{aligned} & \min_{\mathbf{x} \in \{0,1\}^n} \mathbf{x}^T Q \mathbf{x} \\ Q &= -P_0 A^2 \hat{\mathbf{d}} \hat{\mathbf{d}}^T A - P_0 A \hat{\mathbf{d}} \hat{\mathbf{d}}^T A^2 + P_1 C \\ C &= (1 - 2\tau)I + U \end{aligned}$$

with  $\tau = 1$ , where the matrix  $U$  is defined in Eq (9)

using experimental results on several graphs.

### 3 Results and Discussion

#### 3.1 Tools and Implementation

Using Python packages NumPy [38], SciPy [39], D-Wave Ocean [40], IBM Qiskit [41], NetworkX [42], and Matplotlib [43] and the D-Wave 2000Q and IBM Q hardware, we were able to verify the validity of our formulation (proposition 1) for different graphs (see Fig. 6, and Fig. 5) using different values of  $\tau \geq 1$  by comparing our D-Wave 2000Q/IBM-Q output with centrality rankings obtained from the NetworkX EC tool. The QUBO constructed for the EC problem was implemented on the D-Wave 2000Q\_LANL machine at Los Alamos National Laboratory [44] and also on IBM Q using IBM Qiskit QASM simulator or real quantum devices available on the IBM Q, in particular `ibmq_manhattan` [41]. At the front-end of the D-Wave platform, we use D-Wave Ocean tools to submit instructions for the optimal ground state solution for the problem Hamiltonian/QUBO with specified parameters such as the anneal time, chain strength, post-processing method and the number of samples to be collected. The front-end then sends the instructions to the 2000Q\_LANL solver chip for processing. Once the problem Hamiltonian is successfully embedded onto the chip, the annealer solves the QUBO for the minimum energy solution which is a bit string that minimally violates the constraint. Note that the bit string returned has  $\tau$  number of 1's whose corresponding index denote the the top  $\tau$  nodes of the graph. To solve the QUBO problem on the IBM-Q Experience platform, we employed Qiskit's CPLEX tools [45] in generating a quadratic program that is converted to a QUBO/Ising operator for building quantum instances on available QASM simulators or real quantum devices available on the IBM Q. The ground state of the QUBO Hamiltonian is then solved using a Minimum Eigen Solver [46] such as quantum approximate optimization algorithm (QAOA) [47]. Due to qubit limitation, the QUBO can be implemented for graphs with at most 65 nodes on IBM-Q's Manhattan which can encode at most 65 qubits.



### 3.2 Results

Our formulation was examined for several graphs such as shown in Fig. (6) and Fig. (5) on both quantum devices. For our investigations, we examined both fabricated and famous graphs. These graphs were created using the NetworkX graph generator algorithms [48]. The graphs in Fig. (6) include scale-free networks, that is networks with power law or scale-free degree distribution. The Barabasi-Albert graph,  $G_4$ , is an example of a scale-free network which integrates two essential concepts in real networks: growth (increasing number of nodes in the network) and preferential attachment (highly connected nodes have a maximum likelihood of obtaining new connections) [49]. Other well known graphs considered are social networks such as the Davis Southern women social network – the network of a Southern women social club made up of 18 women who attended 14 different events, and the Karate Club graph – network of a university karate club, Bull graph,  $G_{10}$ , complete graphs  $K_n$ , complete bipartite graphs  $K_{m,n}$ , Sedgewick-Maze graph, Barbell graph – two complete graphs joined together by a path graph, (eg. the Lollipop graph,  $G_7$ ), Tutte graph – a cubic polyhedral graph,  $G_3$ , with 46 nodes and 69 edges. The fabricated graphs were mostly tree graphs– connected acyclic undirected graphs such as graphs  $G_1$ , and  $G_8$ . The tree graphs  $G_1$  and  $G_8$  were fabricated mainly to test and show that the QUBO formulation is correctly executing EC rather than a degree centrality measure.

NetworkX was used to obtain initial EC measures and node rankings for comparison with results from the quantum computations on small graphs.

Our analysis started with a careful examination of the formulated unconstrained minimization problem, Eq (6), using classical optimization tools from SciPy [39]. The analysis is aimed at verifying the possibility of constructing an unconstrained optimization problem whose solution determines the EC values of a graph exactly or within a small margin of error and concurrently preserves the node rankings of the graphs before we went on to formulate the quantum version.

Classical minimization using this equation preserved the ranking of the nodes within a small error (see Table 2). This is of small concern however as these nodes have extremely similar values. Therefore, the results obtained using classical minimization in Eq (6) were in support of our hypothesis with the worst case showing the invariance of the rankings in the top 25% of the most central nodes.

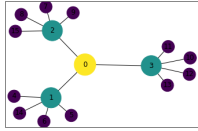
With these results, we moved forward to the construction of a quantum minimization problem:

$$\min_{\mathbf{x} \in \{0,1\}^n} \mathbf{x}^T Q \mathbf{x}$$

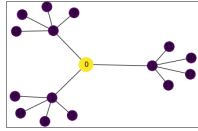
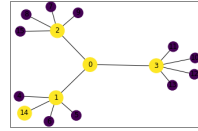
with the objective of identifying the top  $\tau$  most important nodes within our graphs, as confirmed by the results from NetworkX and the classical minimization mentioned previously. Note that here, the goal is to capture the top  $\tau$  most important nodes of the graph irrespective of their order.

Graph $G = (V, E)$ Features				Most central node by EC		Top 5 most central nodes	
Name	$ V $	$ E $	Density $\rho(G)$	Nx	QA	Nx	QA
Bull	5	5	0.5	1	1	0,1,2,3,4	0,1,2,3,4
$K_{3,5}$	8	15	0.54	0,1,2	2	0,1,2,3,4	0,1,2,3,4
$K_5$	5	10	1	-	0	-	-
$K_6 + S_6$	12	18	0.32	5	5	0,1,2,3,4,5	0,1,2,3,5
Florentine Family $F$	15	20	0.19	Medici	Medici	Guadagni, Medici, Ridolfi, Strozzi, Tomabuoni	Guadagni, Medici, Ridolfi, Strozzi, Tomabuoni
Tutte $G_3$	46	69	0.07	-	7	-	12, 30, 36, 44, 45
Lollipop $L_{10,20} = G_7$	30	65	0.15	9	9	0,1,2,4,9	0,1,2,4,9
Barabasi-Albert $BA(50, 5) = G_4$	50	225	0.18	7	7	5,6,7,8,11	•
Davis southern women $G_2$	32	89	0.18	E8	E8	E7,E8,E9, Evelyn Jefferson, Theresa Anderson	E7,E8,E9, Evelyn Jefferson, Theresa Anderson
Karate club	34	78	0.14	33	33	0,1,2,32,33	0,1,2,32,33
Sedgewick-Maze	8	10	0.36	4	4	0,3,4,5,7	0,3,4,5,7
$G_8$ Fig. (5)	16	15	0.13	0	0	0,1,2,3,4	0,1,2,3,8
$G_1$ Fig. (6)	20	19	0.1	1	1	0,1,2,3,5	0,1,2,5,6
$M$ Fig. (5)	13	15	0.19	2	2	0,1,2,6,9	0,1,2,6,9

**Table 1** Table showing the results obtained after implementing the QUBO  $Q$  for  $\tau = 1$  and  $\tau = 5$  on the graphs we considered. The first 4 columns describe some basic graph features such as the name of the graph, number of nodes  $|V|$ , number of edges  $|E|$  and the density of the graph  $\rho = \frac{2|E|}{|V|(|V|-1)}$ . Columns 5 and 6 describe the most central node corresponding to the EC NetworkX result and D-Wave QA result for the QUBO. The last two columns describe the top 5 most central nodes using the EC measure in NetworkX and by implementing the QUBO,  $Q$  on D-Wave (QA). A “-” signifies no node was identified as most central or least central, all node are of the same centrality.



(a) NetworkX ranking

(b) Ranking obtained from IBM-Q and D-Wave for  $\tau = 1$ (c) Ranking obtained on both IBM-Q and D-Wave using  $\tau = 5$ 

**Fig. 2** The graph  $G_8$  showing the most central nodes using the NetworkX EC algorithm (a) and QUBO on IBM-Q and D-Wave quantum computers (Fig. (b) and (c)) for  $P_0 = \frac{1}{\sqrt{n}}$  and  $P_1 = 5n$  where  $n$  is the number of nodes of the graphs. For (a), the most central node(s) is(are) of brighter colors and are encircled by larger circles. In (b) and (c), the bright colored (yellow) nodes are the most central nodes while the dark colored (purple) nodes are the least central nodes relative to  $\tau$ .

Rank	Node	NetworkX	Node	Scipy NM
1	0	0.4629	0	0.4625
2	1	0.4082	3	0.4116
3	2	0.4082	2	0.4075
4	3	0.4082	1	0.4068
5	4	0.1543	12	0.1580
6	5	0.1543	15	0.1563
7	6	0.1543	14	0.1556
8	7	0.1543	4	0.1552
9	8	0.1543	8	0.1546
10	9	0.1543	10	0.1545
11	10	0.1543	9	0.1539
12	11	0.1543	13	0.1538
13	12	0.1543	5	0.1536
14	13	0.1543	6	0.1522
15	14	0.1543	7	0.1513
16	15	0.1543	11	0.1504

**Table 2** NetworkX eigenvector centrality values and node rankings for graph  $G_8$ . The result was obtained using the SciPy minimizer with the Nelder-Mead method in solving Eq.(6). The column titled “Rank”, defines the rank on each node in the columns titled “Nodes” using the centrality values obtained from both methods.

Experimenting with the QUBO Eq (11) on both the D-Wave 2000Q and IBM-Q devices (QASM simulator and `ibmq_manhattan` for the Karate club graph), we obtained results showing that the formulation indeed captures EC and not degree centrality ranking when compared with the NetworkX output. Fig. (2b) shows the output for a search for the most central node (colored yellow) which in this case requires  $\tau = 1$  of the graph  $G_8$  in Fig. (5). Compared to the NetworkX output in Fig. (5a), the quantum computing scheme supports proposition 1, the claim that the ground state of the QUBO encapsulates the information about the nodes with high ranked EC values and not those of high ranked degree centrality values. Fig. (2c), shows the result obtained for a search for the top  $\tau = 5$  most important nodes (in yellow) of the graph  $G_8$ . For the NetworkX results, the most central nodes are identified by the size and brightness of the color of the disk around the nodes; the larger and brighter the disk the more central the node. For the graph  $G_8$ , the yellow node (0) is the most central, followed by nodes 1, 2, 3 and the nodes 4, 5, 6, . . . , 14 are all of the same centrality value and are the least central nodes. It was observed that it is sufficient to choose the penalty constants  $P_0 = \frac{1}{\sqrt{n}}$ , and  $P_1 > P_0$  (in our case  $P_1 = 5n$  worked well).

To obtain optimal results using the D-Wave 2000Q, it is best to set the chain strength to the maximum possible, 1000 in this case. It was observed that very low chain strength values resulted in broken chains affecting the probability of the QA settling into a global minimum solution. Setting the post-processing method to “optimization” and the number of samples to the maximum, 10,000 boosted the chances of obtaining the optimal solution. However as the graph gets larger more samples are required to increase the probability of observing the ground state solution. Here is where some inconsistencies in

obtaining the lowest energy output for larger graphs was highlighted: the first (or second, etc.) run may not result in the expected output. Running multiple times would eventually result in the correct output occurring once, but due to the noisy and quantum nature of the quantum machine, we do not know the exact number of runs required to give the global minimum solution. This was mostly observed in the Karate Club graph in Fig. (3e) and the Davis Southern women network. With a little bit of luck the result can be obtained in the first run or in a few runs. This behavior is not surprising since an increase in the problem size decreases the probability of finding an optimal solution due to annealing error and imperfect hardware[50].

The quadratic solver QBSolv in Ocean served as a benchmark for determining the correct minimum of the D-Wave annealing output. QBSolv provided expected results of the minimization on most occasions with degenerate ground state solutions in some instances. Degeneracy here refers to the outputs with the same minimum energy value of the QUBO due to multiple nodes having the same centrality value. Whenever there is degeneracy in the QBSolv output, one of the solutions correctly identifies the top  $\tau$  nodes. For example, in Fig. (2c), we have 12 degenerate solutions corresponding to the 12 leaves of the tree graph. The solution graphed included node 14 in the top 5 important nodes, however node 4, 5, 6, 7, 8, 9, 10, 11, 12, 13 or 15 are valid replacements for node 14 in this output since column 3 of Table 2 shows that all these nodes have same centrality values.

Solving the problem for the QUBO in Eq. (11) for the graph in Fig. (1) and graph  $G_8$  in Fig. (6) correctly identify the most important nodes for any given  $\tau$ , including selecting node 0 as the node with the highest EC (see Fig. (2)). The penalty weights used here were  $P_0 = \frac{1}{\sqrt{n}}$  and  $P_1 = 5n$  for  $n$  number of nodes of the graphs. The same results were obtained from experiments on IBM-Q's QASM simulator using QAOA. However the ground state solution for the graphs with smaller numbers of nodes ( $n \leq 16$ ) were obtained on a single run with the penalty constants  $P_0 = \frac{1}{\sqrt{n}}$  and  $P_1 = 5n$ . When considering graphs with larger numbers of nodes, the program had to be run multiple times using the same penalty constants above to be able to capture the global minimum solution.

Solving for the ground state solution of the QUBO in Eq. (11) for the graph  $G_1$  and Karate Club graph in Fig. (6) was quite challenging. On most occasions, the solution for the Karate Club graph with  $\tau \geq 3$  required multiple runs before settling on the global minimum solution. In other words, this graph required more samples to be able to output the global minimum. For  $3 \leq \tau \leq 5$ , the QUBO couldn't capture the ordering that matched that of NetworkX rankings when using the penalty constants  $P_0 = \frac{1}{\sqrt{n}}$  and  $P_1 = 5n$  for the graph  $G_1$ . The nodes 0, 3, 4 were always skipped in the search for the top  $\tau = 3, 4, 5$ . From Fig. (3d), we see that the output for the top 6 most important nodes excludes node 4 and includes node 2 which shouldn't be the case since from Fig. (3a), node 4 is more central than node 2. The exact reason for this occurrence for this particular graph is unknown, however it seems the

program picks only one of the degenerate nodes 3, or 4 and moves on to select the next central node 2.

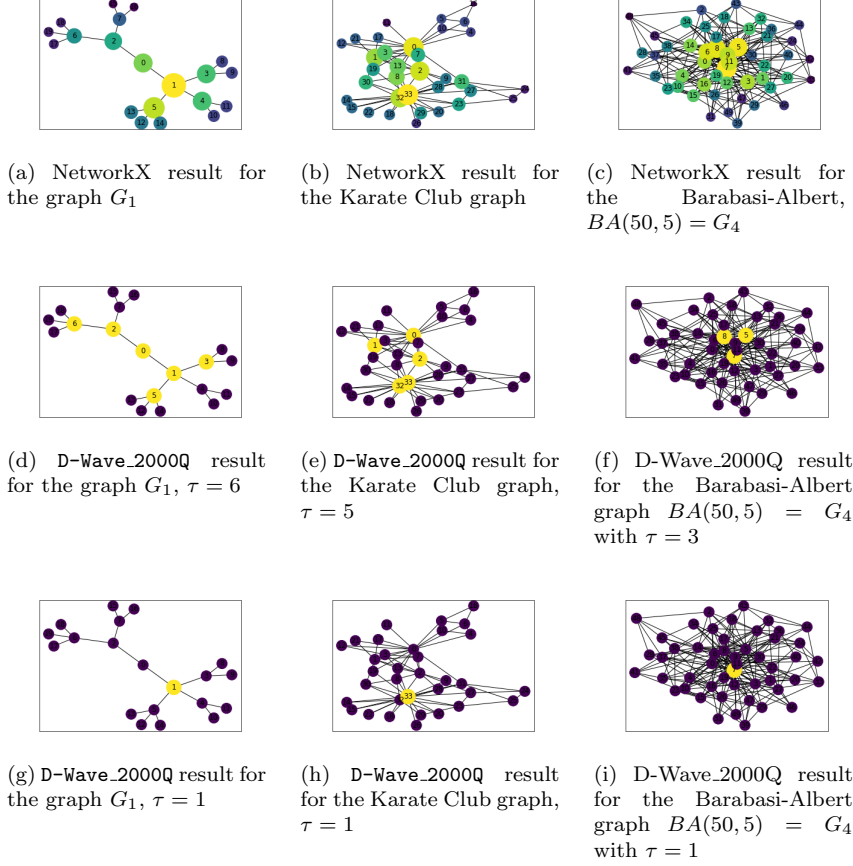


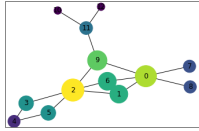
**Fig. 3** Top:NetworkX results for the challenging graphs encountered and Bottom: Results from running on D-Wave for  $P_0 = \frac{1}{\sqrt{n}}$  and  $P_1 = 5n$  using the QUBO in Eq. 11. The D-Wave results colors the top  $\tau$  most important nodes yellow and the least central nodes purple. The NetworkX result identifies most central nodes with larger and brighter circles (yellow being the top) and least central nodes with smaller and darker circles (least being purple).

With these interesting results, we further examined the possibility of defining a hierarchy of nodes in the network from the QUBO results obtained from the D-Wave 2000Q and IBM Q. By hierarchy we mean a ranking that orders the nodes based on importance or influence using EC. The hierarchy can then be used to identify for example super-spreaders of disease. We compare the hierarchy of nodes obtained using our QUBO formulation with that obtained from NetworkX when using the EC algorithm. The result obtained for graph  $M$

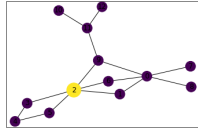
$\tau$	(QA/QAOA) QUBO results for top $\tau$ most central nodes of graph $M$	Node Rank of (QA/QAOA) QUBO results for $M$	Node Rank of NetworkX EC result for $M$
1	2	2	2
2	0, 2	0	0
3	0, 2, 9	9	9
4	0, 1, 2, 9	1	1
5	0, 1, 2, 6, 9	6	6
6	0, 1, 2, 3, 6, 9	3	3
7	0, 1, 2, 3, 5, 6, 9	5	5
8	0, 1, 2, 3, 5, 6, 9, 11	11	11
9	0, 1, 2, 3, 4, 5, 6, 9, 11	4	7
10	0, 1, 2, 3, 4, 5, 6, 7, 9, 11	7	8
11	0, 1, 2, 3, 4, 5, 6, 7, 8, 9, 11	8	4
12	0, 1, 2, 3, 4, 5, 6, 7, 8, 9, 11, 12	12	10
13	0, 1, 2, 3, 4, 5, 6, 7, 8, 9, 10, 11, 12	10	12

**Table 3** Determining node rank from the QUBO result obtained from D-Wave (QA) and IBM-Q (QAOA) using symmetric difference of results for  $\tau = 1$  to  $\tau = n$ . In column 4, the  $i$ th in rank is determined by taking the difference of the result for  $\tau = i$  and  $\tau = i - 1$  e.g. the 1st (most central) node 2 is determined by implementing the QUBO for  $\tau = 1$ , the 2nd is determined by taking the difference between the result of  $\tau = 2$ ,  $\{0, 2\}$  and the result of  $\tau = 1, \{2\}$ , i.e.  $\{0, 2\} \setminus \{2\} = \{0\}$ , implying node 0 is ranked second in importance.

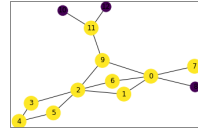
is shown in Table 3. To determine the node rank, we consider the set of  $\tau$  nodes obtained from the QUBO results for each value of  $0 < \tau \leq n$  and compute the symmetric difference. The  $i$ th rank is determined by taking the difference of the QUBO result for  $\tau = i$  and  $\tau = i - 1$ . For example, to rank the nodes for graph  $M$ , the 1st most important node is obtained by running the QUBO for  $\tau = 1$ . The 2nd most important node is determined by taking the difference between the QUBO results for  $\tau = 2$ ,  $\{0, 2\}$  and the result  $\{2\}$  of  $\tau = 1$ . Thus  $\{0, 2\} \setminus \{2\} = \{0\}$  implies that node 0 is the second most important node. Continuing in this manner the importance of the nodes can be ranked. Computing the difference  $\{0, 1, 2, 3, 4, 5, 6, 7, 9, 11\} \setminus \{0, 1, 2, 3, 4, 5, 6, 9, 11\} = \{7\}$  for  $\tau = 10$  and  $\tau = 9$  we see that the 10th important node is node 7.



(a) NetworkX ranking



(b) Ranking obtained from IBM-Q and D-Wave for  $\tau = 1$



(c) Ranking obtained from IBM-Q and D-Wave using  $\tau = 10$

**Fig. 4** The graph  $M$  showing the most central nodes using the NetworkX EC algorithm (a) and QUBO on the IBM-Q and D-Wave quantum computers (Fig. (b) and (c)) for  $P_0 = \frac{1}{\sqrt{n}}$  and  $P_1 = 5n$  where  $n$  is the number of nodes of the graphs. For (a), the most central node(s) is(are) of brighter colors and are encircled by larger circles. In (b) and (c), the bright colored (yellow) nodes are the most central nodes while the dark colored (purple) nodes are the least central nodes relative to  $\tau$ .

## 4 Conclusion

We have formulated and shown a QUBO problem for the identification of most important nodes or hot-spots in a graph based on the EC measure is possible. Using quantum computing algorithms such as quantum annealing on the D-Wave 2000Q and QAOA on IBM-Q, our formulation was able to correctly identify all  $\tau < n$  most important nodes for graphs with less than 17 nodes ( $n < 17$ ). For graphs with more than 16 nodes, the quantum computing algorithm always identified the top  $\tau \leq 6$  most important nodes for all the graphs considered correctly except for the Davis Southern women network and the tree graph  $G_1$  whose outputs for some values of  $1 < \tau \leq 6$  showed some marginal inconsistencies. Marginal because the differences are negligible. For example, for the graph  $G_1$ , the node 3 was not selected since its centrality value is the same as that of node 4. Despite this challenge, the results obtained from all graphs considered for  $\tau = 1$  verified Proposition 1. We have also demonstrated the feasibility of defining a hierarchy of nodes in a graph from our formulation using the QUBO results from D-Wave 2000Q and IBM-Q's QASM simulator. Given that the current quantum resources (D-Wave 2000Q and IBM-Q's Manhattan ) at our disposal limit us on the size of graphs to explore and in the presence of uncontrollable noise which affects the probabilities of obtaining quality results, we were unable to experiment with real life data. Therefore in the future when powerful and less noisy quantum computers are made available for our perusal, we wish to test our hypothesis further to establish a more generalized formulation that works for all  $\tau$  on all graphs. That is, we want to verify

*Claim* For any graph  $G = (V, E)$ , with adjacency matrix  $A$  and degree sequence  $D$ . The indices of the nonzero elements of the ground state solution to the QUBO problem

$$\begin{aligned} & \min_{\mathbf{x} \in \{0,1\}^n} \mathbf{x}^T Q \mathbf{x} \\ Q &= -P_0 A^2 \hat{\mathbf{d}} \hat{\mathbf{d}}^T A - P_0 A \hat{\mathbf{d}} \hat{\mathbf{d}}^T A^2 + P_1 C \\ C &= (1 - 2\tau)I + U \end{aligned}$$

where the matrix  $U$  is defined in Eq. (9), corresponds to the  $\tau$  most central nodes via EC measure of the graph  $G$  for any  $\tau \leq n = |V|$ .

For this claim we wish to investigate both directed and undirected graphs, "will replacing  $A^2$  by  $AA^T$  or  $A^T A$  in  $Q$  still work for directed graphs or will it require a modified QUBO?"

## Appendix A : Computing Degree Centrality and Eigencentality from Exponential Function

Consider the exponential function defined by

$$f(x) = e^x = \sum_{k=0}^{\infty} \frac{x^k}{k!} \quad (13)$$

Since  $f$  is continuous and analytic with radius of convergence infinity, we observe that for a primitive matrix  $A$  which is mostly the case for the adjacency matrix of simply connected undirected graphs

$$f(\gamma A) = e^{\gamma A} = \sum_{k=0}^{\infty} \frac{(\gamma A)^k}{k!} \quad (14)$$

Then  $f(\gamma A)$  is a matrix and the components of the vector  $f(\gamma A)\mathbf{1}$  where  $\mathbf{1}$  is a vector of ones, counts the walks of infinite length centered at each node. Let  $\{\mathbf{e}_i \in \mathbb{R}^n\}$  be the set of canonical basis vectors for  $\mathbb{R}^n$  whose only nonzero element is the  $i$ th component.

$$\begin{aligned} v_i(\gamma) &= \sum_{j=0}^{n-1} \mathbf{e}_i^T f(\gamma A) \mathbf{e}_j \\ &= \sum_{k=0}^{\infty} \sum_{j=0}^{n-1} \mathbf{e}_i^T \frac{(\gamma A)^k}{k!} \mathbf{e}_j \\ &= \sum_{k=0}^{\infty} \sum_{j=0}^{n-1} a_k \gamma^k \mathbf{e}_i^T A^k \mathbf{e}_j \\ &= a_0 \sum_{j=0}^{n-1} \mathbf{e}_i^T \mathbf{e}_j + a_1 \gamma \sum_{j=0}^{n-1} \mathbf{e}_i^T A \mathbf{e}_j + \dots \\ &= a_0 + a_1 \gamma d_i + \sum_{k=2}^{\infty} \sum_{j=0}^{n-1} a_k \gamma^k \mathbf{e}_i^T A^k \mathbf{e}_j \\ c_i(\gamma) &= \frac{v_i(\gamma) - a_0}{a_1 \gamma} = d_i + \sum_{k=2}^{\infty} \sum_{j=0}^{n-1} \frac{a_k}{a_1} \gamma^{k-1} \mathbf{e}_i^T A^k \mathbf{e}_j \end{aligned} \quad (15)$$

where  $d_i$  is the degree of the  $i$ th node. In the limit  $\gamma \rightarrow 0^+$ , Eq. (15) converges to the degree centrality and by expanding in the eigenbasis, it converges to EC for  $\gamma \rightarrow \infty$  [10].

## Appendix B : Graphs Considered



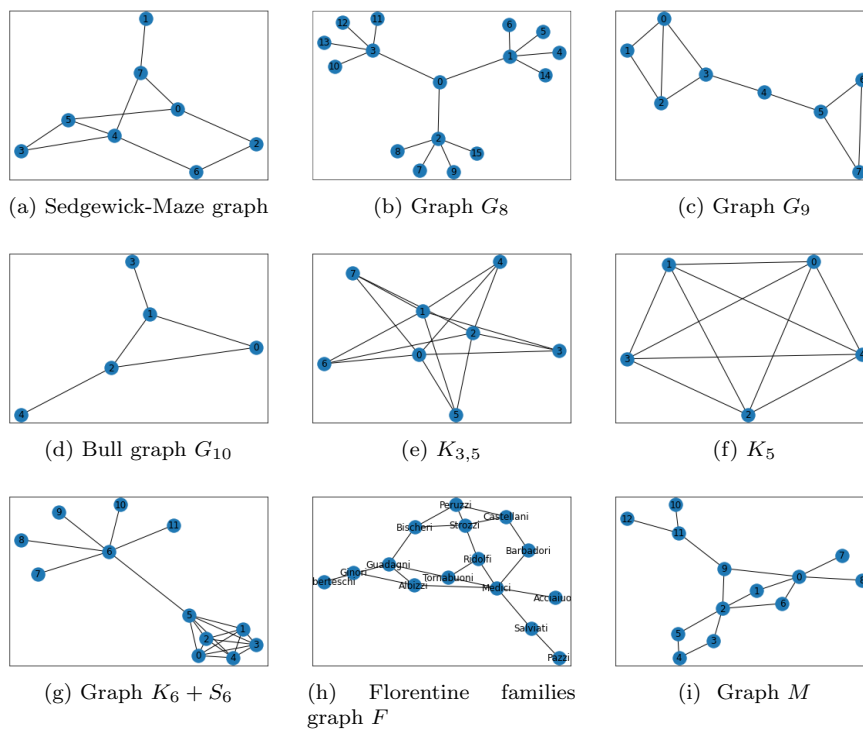


Fig. 5 Some graphs with smaller number of nodes considered

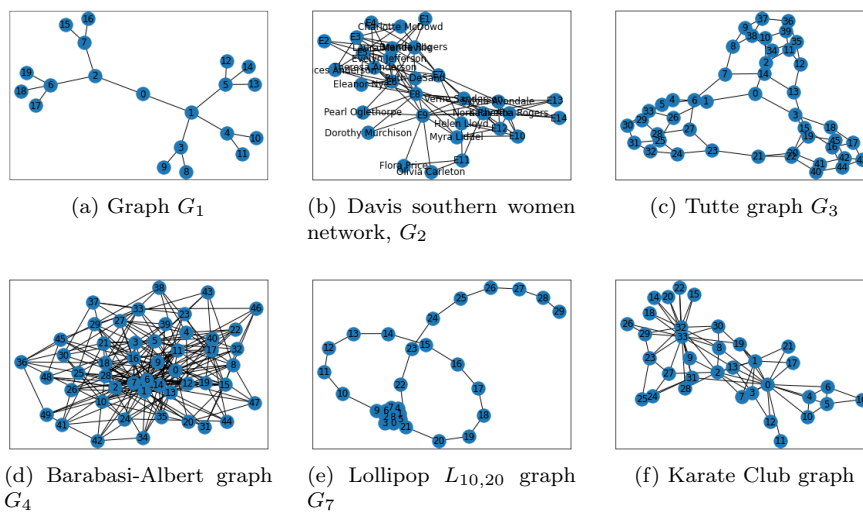


Fig. 6 Samples of graphs with larger number of nodes considered

**Acknowledgements** Research presented in this article was supported by the Laboratory Directed Research and Development (LDRD) program of Los Alamos National Laboratory (LANL) under project number 20200056DR. LANL is operated by Triad National Security, LLC, for the National Nuclear Security Administration (NNSA) of the U. S. Department of Energy (contract no. 89233218CNA000001). TJ acknowledges support from the U.S. Department of Energy (DOE) through a quantum computing program sponsored by the Los Alamos National Laboratory (LANL) Information Science & Technology Institute. This research was also supported by the U. S. Department of Energy (DOE) National Nuclear Security Administration (NNSA) Advanced Simulation and Computing (ASC) program at LANL. We acknowledge the ASC program at LANL for use of their Ising D-Wave 2000Q quantum computing resource. Quantum resources from the IBM-Q Hub are also acknowledged. Assigned: Los Alamos Unclassified Report LA-UR-21-24030.

## Conflict of interest

The authors declare that they have no conflict of interest.

## References

1. L. C. Freeman, "Centrality in social networks conceptual clarification," *Social Networks*, vol. 1, no. 3, pp. 215–239, 1978-1979.
2. G. Sabidussi, "The centrality index of a graph," *Psychometrika*, vol. 31, pp. 581–603, 1966.
3. E. Chea and D. R. Livesay, "How accurate and statistically robust are catalytic site predictions based on closeness centrality?," *Bmc Bioinformatics*, vol. 8, no. 1, pp. 1–14, 2007.
4. L. C. Freeman, "A set of measures of centrality based on betweenness," *Sociometry*, vol. 40, no. 1, pp. 35–41, 1977.
5. H. Yu, P. M. Kim, E. Sprecher, V. Trifonov, and M. Gerstein, "The importance of bottlenecks in protein networks: correlation with gene essentiality and expression dynamics," *PLoS Comput Biol*, vol. 3, no. 4, p. e59, 2007.
6. L. Katz, "A new status index derived from sociometric index," *Psychometrika*, pp. 39–43, 1953.
7. J. Zhao, T.-H. Yang, Y. Huang, and P. Holme, "Ranking candidate disease genes from gene expression and protein interaction: a katz-centrality based approach," *PloS one*, vol. 6, no. 9, p. e24306, 2011.
8. S. Brin and L. Page, "The anatomy of a large-scale hypertextual web search engine," *Computer Networks and ISDN Systems*, vol. 30, no. 1-7, pp. 107–117, 1998.
9. M. Benzi and C. Klymko, "Total communicability as a centrality measure," *Journal of Complex Networks*, vol. 1, no. 2, p. 124–149, 2013.
10. M. Benzi and C. Klymko, "On the limiting behavior of parameter-dependent network centrality measures," *SIAM Journal on Matrix Analysis and Applications*, vol. 36, no. 2, pp. 686–706, 2015.
11. D. Schoch, T. W. Valente, and U. Brandes, "Correlations among centrality indices and a class of uniquely ranked graphs," *Social Networks*, vol. 50, pp. 46–54, 2017.

12. J. R. F. Ronqui and G. Travieso, "Analyzing complex networks through correlations in centrality measurements," *Journal of Statistical Mechanics: Theory and Experiment*, vol. 2015, p. P05030, may 2015.
13. M. Mihail and C. Papadimitriou, "On the eigenvalue power law," in *Randomization and Approximation Techniques in Computer Science. RANDOM 2002*, pp. 254–262, Springer, Berlin, Heidelberg, 06 2002.
14. P. Bonacich, "Power and centrality: A family of measures," *American Journal of Sociology*, vol. 92, no. 5, pp. 1170–1182, 1987.
15. C. Negre, U. Morzan, H. Hendrickson, R. Pal, G. Lisi, J. Loria, I. Rivalta, J. Ho, and V. Batista, "Eigenvector centrality for characterization of protein allosteric pathways," *Proc Natl Acad Sci USA*, vol. 115, no. 52, pp. E12201–E12208, 2018.
16. J. Jimenez-Martinez and C. F. A. Negre, "Eigenvector centrality for geometric and topological characterization of porous media," *Phys. Rev. E*, vol. 96, p. 013310, Jul 2017.
17. S. Azad and S. Devi, "Tracking the spread of covid-19 in india via social networks in the early phase of the pandemic," *Journal of Travel Medicine*, vol. 27, December 2020.
18. G. B. Navaretti, G. Calzolari, A. Dossena, A. Lanza, and A. F. Pozzolo, "In and out lockdowns: Identifying the centrality of economic activities," *Covid Economics*, vol. 17, pp. 189–204, 2020.
19. M. Newman, *Networks*. OUP Oxford, 2018.
20. O. Perron, "Zur theorie der matrices," *Math. Ann.*, vol. 64, p. 248–263, 1907.
21. "Quantum computing in a nutshell," 2021. Online; accessed March 9, 2021.
22. "Welcome to d-wave," 2020. Online; accessed February 2, 2021.
23. "D-wave qpu architecture: Chimera," 2020. Online; accessed December 25, 2020.
24. "Minor-embedding a problem onto the qpu," 2020. Online; accessed December 21, 2020.
25. J. P. Terry, P. D. Akrobotu, C. F. A. Negre, and S. M. Mniszewski, "Quantum isomer search," *PLoS ONE*, vol. 15, no. 1, 2020.
26. H. Ushijima-Mwesigwa, C. F. A. Negre, and S. M. Mniszewski, "Graph partitioning using quantum annealing on the d-wave system," in *Proceedings of the Second International Workshop on Post Moores Era Supercomputing*, PMES'17, (New York, NY, USA), pp. 22–29, ACM, 2017.
27. C. F. A. Negre, H. Ushijima-Mwesigwa, and S. M. Mniszewski, "Detecting multiple communities using quantum annealing on the d-wave system," *PLoS ONE*, vol. 15, no. 2, 2020.
28. C. Bauckhage, E. Brito, K. Cvejovski, C. Ojeda, R. Sifa, and S. Wrobel, "Ising models for binary clustering via adiabatic quantum computing," in *Energy Minimization Methods in Computer Vision and Pattern Recognition* (M. Pelillo and E. Hancock, eds.), (Cham), pp. 3–17, Springer International Publishing, 2018.

29. C. S. Calude, M. J. Dinneen, and R. Hua, "Qubo formulations for the graph isomorphism problem and related problems," *Theoretical Computer Science*, vol. 701, pp. 54–69, 2017. At the intersection of computer science with biology, chemistry and physics - In Memory of Solomon Marcus.
30. K. Pudenz and D. Lidar, "Quantum adiabatic machine learning," *Quantum Inf Process*, vol. 12, p. 2027–2070, 2013.
31. S. H. Adachi and M. P. Henderson, "Application of Quantum Annealing to Training of Deep Neural Networks," *arXiv e-prints*, p. arXiv:1510.06356, Oct. 2015.
32. V. Carnevali, I. Siloi, R. Di Felice, and M. Fornari, "Vacancies in graphene: an application of adiabatic quantum optimization," *Phys. Chem. Chem. Phys.*, vol. 22, pp. 27332–27337, 2020.
33. D. Venturelli, D. J. J. Marchand, and G. Rojo, "Quantum Annealing Implementation of Job-Shop Scheduling," 2016.
34. T. Stollenwerk, E. Lobe, and M. Jung, "Flight gate assignment with a quantum annealer," in *Quantum Technology and Optimization Problems* (S. Feld and C. Linnhoff-Popien, eds.), (Cham), pp. 99–110, Springer International Publishing, 2019.
35. T. Stollenwerk, B. O’Gorman, D. Venturelli, S. Mandrà, O. Rodionova, H. Ng, B. Sridhar, E. G. Rieffel, and R. Biswas, "Quantum annealing applied to de-conflicting optimal trajectories for air traffic management," *IEEE Transactions on Intelligent Transportation Systems*, vol. 21, no. 1, pp. 285–297, 2020.
36. K. Michielsen, M. Nocon, D. Willsch, F. Jin, T. Lippert, and H. De Raedt, "Benchmarking gate-based quantum computers," *Computer Physics Communications*, vol. 220, pp. 44–55, 2017.
37. "Quantum computing software and programming tools," 2009. Online; accessed April 22, 2021.
38. "Numpy," 2020. Online; accessed December 25, 2020.
39. "Scipy," 2020. Online; accessed December 25, 2020.
40. "D-wave’s ocean software," 2020. Online; accessed December 25, 2020.
41. "Qiskit," 2020. Online; accessed December 25, 2020.
42. A. A. Hagberg, D. A. Schult, and P. J. Swart, "Exploring network structure, dynamics, and function using networkx," in *Proceedings of the 7th Python in Science Conference (SciPy 2008)*, SciPy 2008, pp. 11–16, ACM, 2008.
43. J. D. Hunter, "Matplotlib: A 2d graphics environment," *Computing in Science & Engineering*, vol. 9, no. 3, pp. 90–95, 2007.
44. "Los alamos national laboratory upgrades to d-wave 2000q™ quantum computer," 2019. Online; accessed December 24, 2020.
45. "Converters for quadratic programs," 2020. Online; accessed December 26, 2020.
46. "Minimum eigen optimizer," 2020. Online; accessed December 26, 2020.
47. E. Farhi, J. Goldstone, and S. Gutmann, "A quantum approximate optimization algorithm," 2014.
48. "Graph generators," 2020. Online; accessed March 9, 2021.

- 
49. Wikipedia contributors, “Barabási–albert model — Wikipedia, the free encyclopedia,” 2021. [Online; accessed 27-January-2021].
  50. K. L. Pudenz, T. Albash, and D. A. Lidar, “Quantum annealing correction for random ising problems,” *Physical Review A*, vol. 91, no. 4, p. 042302, 2015.